


Review

# Review of Specialty Fiber Based Brillouin Optical Time Domain Analysis Technology

Dora Juan Juan Hu <sup>1,\*</sup> , Georges Humbert <sup>2</sup>, Hui Dong <sup>1</sup>, Hailiang Zhang <sup>1</sup>, Jianzhong Hao <sup>1</sup> and Qizhen Sun <sup>3</sup>

<sup>1</sup> Institute for Infocomm Research, Agency for Science, Technology and Research, Singapore 138632, Singapore; hdong@i2r.a-star.edu.sg (H.D.); Zhang\_Hailiang@i2r.a-star.edu.sg (H.Z.); haoemily@i2r.a-star.edu.sg (J.H.)

<sup>2</sup> XLIM Research Institute, UMR CNRS/University of Limoges, 123 Av. Albert Thomas, 87060 Limoges, France; georges.humbert@xlim.fr

<sup>3</sup> School of Optical and Electronic Information & National Engineering Laboratory for Next Generation Internet Access System (NGIA) & Wuhan National Laboratory for Optoelectronics (WNLO), Huazhong University of Science and Technology, Wuhan 430074, China; qzsun@mail.hust.edu.cn

\* Correspondence: jjhu@i2r.a-star.edu.sg

**Abstract:** Specialty fibers have introduced new functionalities and opportunities in distributed fiber sensing applications. Particularly, Brillouin optical time domain analysis (BOTDA) systems have leveraged the unique features of specialty fibers to achieve performance enhancement in various sensing applications. This paper provides an overview of recent developments of the specialty fibers based BOTDA technologies and their sensing applications. The specialty fibers based BOTDA systems are categorized and reviewed based on the new features or performance enhancements. The prospects of using specialty fibers for BOTDA systems are discussed.

**Keywords:** specialty fibers; Brillouin optical time domain analysis; BOTDA; distributed fiber sensor; photonic crystal fiber; strain and temperature sensing



**Citation:** Hu, D.J.J.; Humbert, G.; Dong, H.; Zhang, H.; Hao, J.; Sun, Q. Review of Specialty Fiber Based Brillouin Optical Time Domain Analysis Technology. *Photonics* **2021**, *8*, 421. <https://doi.org/10.3390/photonics8100421>

Received: 23 July 2021

Accepted: 26 September 2021

Published: 30 September 2021

**Publisher's Note:** MDPI stays neutral with regard to jurisdictional claims in published maps and institutional affiliations.



**Copyright:** © 2021 by the authors. Licensee MDPI, Basel, Switzerland. This article is an open access article distributed under the terms and conditions of the Creative Commons Attribution (CC BY) license (<https://creativecommons.org/licenses/by/4.0/>).

## 1. Introduction

Novel specialty optical fibers with engineered materials or specially designed structures have enabled new opportunities to explore novel functionalities and applications. One of the successful applications is in the Brillouin optical time domain analysis (BOTDA) systems, which has emerged as a fast-developing distributed fiber sensor technology for measuring temperature and strain in the past two decades. The capability of distributed strain and temperature measurement and the benefits of a fiber optic sensor system have made the BOTDA systems a favorable solution for long term structural health monitoring (SHM) and assessment of infrastructure. The correlation of strain data and structural health assessment have been investigated and implemented for practical SHM applications, such as damage detection of operating tunnels-based cross-section curvature [1], blade structural fatigue damage of wind turbine [2], structural crack identification and early detection [3], etc. A few examples of field significant applications in the real world are presented in [4], including SHM monitoring in civil infrastructures, such as bridges and railways, geotechnical structures monitoring and pipeline monitoring, etc. Design considerations of BOTDA systems could be from the interrogator to address the technology challenges and meet the performance requirements in spatial resolution, sensing range and dynamic measurement, which are well summarized in several reviews [5–9]. Alternatively, the design can be from the perspectives of fibers or fiber cables. In particular, the exploration of different stimulated Brillouin scattering (SBS) materials and their applications are thoroughly reviewed in [10]. The perspectives of fiber manufacturers on fiber materials and their effects on the Brillouin scattering properties and system designs are presented in [11]. The research and application regarding optical fiber cables for Brillouin distributed sensing are reviewed in [12], showing successful exploitation of the Brillouin sensing technique

using appropriate fiber cable designs. Moreover, post-processing using image processing techniques [13] or machine learning techniques have been reported to improve sensor performance without hardware modification [14].

This paper intends to provide a comprehensive review on the different sensing features and performance enhancements provided by the specialty fibers that are used in BOTDA systems. This paper will cover new developments that were reported after the previous papers, which presented specialty fibers in Brillouin based sensing systems [11,15]. The principle of BOTDA technology is introduced in Section 2, followed by a discussion of the specialty fiber based BOTDA with enhanced sensing capability and performance in Section 3. Firstly, the sensor performance enhancements and breakthroughs are introduced, such as latest breakthroughs in Brillouin amplifications in gas filled hollow-core fibers, sensitivity enhancement and suppression of polarization noise. Secondly, the discriminative sensing of temperature and strain using several techniques are reviewed. Thirdly, multiplexed sensing systems of BOTDA and other distributed fiber sensor (DFS) technologies are reviewed. Fourthly, distributed sensing of other parameters, such as curvatures, pressure and salinity, etc., are reviewed. Lastly, the prospects of using specialty fibers for BOTDA systems are discussed in Section 4.

## 2. Principle of BOTDA Technology

Typical BOTDA systems are based on Brillouin interaction between a pulsed pump and a counter-propagating continuous wave (CW) probe (Figure 1). The probe wave is amplified through SBS process when the frequency difference between the pulsed and the CW light is turned to the Brillouin frequency of the fiber [16]. The probe power is measured as a function of time, which is translated to a distance-dependent information to derive local Brillouin gain. The local Brillouin frequency shift (BFS) at each point of the fiber is derived from reconstruction of the Brillouin gain spectrum (BGS) by a frequency sweep with every frequency detuning around the Brillouin frequency. Both temperature and strain contribute to BFS variations.

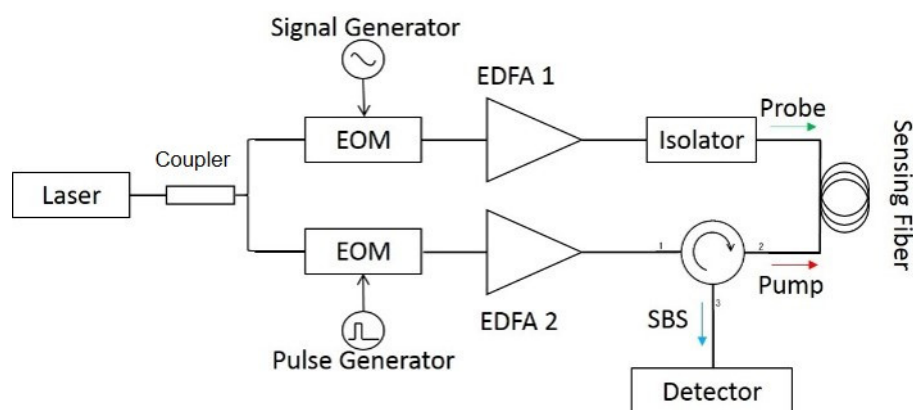


Figure 1. Basic layout of a BOTDA system.

Specialty fibers such as PCFs and hollow-core fibers contain holey structures, which provide an ideal platform to integrate with high gain SBS medium to boost the overall Brillouin amplification. Peculiar Brillouin scattering features of specialty fibers are leveraged to improve the sensor performance of BOTDA systems, such as polarization noise suppression, enhancement of sensitivity, etc. The temperature-compensated distributed strain measurement, or discriminating the response from temperature and strain, is a key challenge in the BOTDA solutions. To overcome this challenge, various specialty fibers have been introduced to the BOTDA solution, such as photonic crystal fibers (PCFs), few mode fibers (FMFs) and multicore fibers etc., which are reviewed in this paper. In addition, multiplexed distributed sensing that consists of the BOTDA technology and other DFS technology, e.g., Raman optical time domain reflectometry (R-OTDR) or phase-sensitive

optical time domain reflectometry ( $\varphi$ -OTDR), are reported based on multi-core fibers via spatial multiplexing. The aforementioned opportunities have generated substantial interest and driven the advancement of the specialty fiber based BOTDA systems with favorable features and performance enhancements as reviewed in the next section.

### 3. Reviews on Specialty Fiber Based BOTDA Technology

Through the design of optical fiber structures and engineering of the optical fiber materials, specialty fibers have offered abundant opportunities in bringing new features, functionalities in fiber devices and enabling new applications. In BOTDA systems, the Brillouin gain spectrum can be customized and optimized through the selection of fiber materials and the design of optical and acoustic waveguide properties in specialty fibers [11]. In this section, a comprehensive review of the specialty fiber based BOTDA with enhanced sensing capability and performance is presented.

#### 3.1. Sensor Performance Enhancements and Breakthroughs

PCF provides a flexible platform to engineer the optical and acoustic waveguide properties to achieve enhanced or reduced Brillouin gain. Brillouin gain in PCFs can be significantly increased by using high Brillouin gain materials as fiber materials or infiltrating high Brillouin gain materials, such as gases, into the holey structure of the PCF. The Brillouin scattering properties and the BGS can be influenced by fiber configurations, fiber material designs and the dopants into the silica glass [11]. The Brillouin gain coefficients of a chalcogenide glass microstructured single mode fiber (SMF) was 100 times larger than fused silica [17]. More recently, a gas-filled hollow-core PCF has demonstrated highly nonlinear Brillouin gain, which scales with the square of the gas pressure and achieved a strain-free high performance distributed temperature sensing [18,19]. On the contrary, solid core PCFs have demonstrated reduced Brillouin gain and a three-fold increase of the Brillouin threshold power with a uniform all-silica fiber. They could be exploited for suppression of Brillouin scattering [20]. Anti-resonant hollow-core fibers exhibited at least three (five if evacuated) orders of magnitude weaker Brillouin scattering compared with conventional SMFs, paving the way to explore ultra-low noise applications for quantum information processing and optical communication [21].

In addition to fiber design and material engineering, the fiber sensing cable design and fiber coatings play a significant role in optimizing the Brillouin distributed fiber sensor performance [12]. For example, SMF with single-layer and double-layer polymer coatings have been used to demonstrate enhanced hydrostatic pressure sensitivities through pressure-induced strain measurement based on Lamé formula. The pressure sensitivity is enhanced by increasing the outer coating radius or decreasing the outer coating Young's modulus and Poisson's ratio. The maximum pressure sensitivity of the double-coated SMF is about five times higher than the single-coated SMF [22]. Similarly, enhanced temperature sensitivity can be achieved by putting optical fibers into suitable coatings [23,24].

Polarization effects on the SBS in PCFs have demonstrated interesting properties. In small core single mode PCFs, a higher SBS threshold of 3 dB is observed due to unintentional birefringence as a result of the asymmetry in the fiber structure geometry as well as the large index contrast. In addition, strong polarization dependence of Brillouin gain has been reported. In particular, the SBS has a strong dependence on pump polarization. The minimum and maximum SBS are 3 dB different and 90° apart. For lower powers below threshold, the transmission presents a 180° polarization periodicity due to polarization dependent losses (PDL). For higher powers above threshold, the transmission shows a 90° polarization periodicity such as SBS as PDL becomes negligible [25]. A large-controlled birefringence could be introduced in these fibers to suppress SBS effect for potential applications that are limited by SBS.

### 3.2. Discriminative Sensing of Temperature and Strain

Discriminative sensing of temperature and strain is an important and desirable capability in BOTDA systems because the optical fiber and its BGS are subject to changes in both parameters. Besides the usage of two independent fibers [26], various approaches have been proposed and demonstrated for achieving this purpose, including approaches to form a sensor matrix, and other approaches based on a combination of using Brillouin scattering and other parameters.

The below sensor matrix (Equation (1)) can be used to describe the sensing system, where the  $C_{T1,2}$  and  $C_{\epsilon1,2}$  represent the temperature and strain coefficients,  $\Delta\nu_{B\_peak1,2}$  represent the central frequency shifts of the Brillouin spectra peaks. By solving the inverse matrix problem, distributed measurement of the temperature change  $\Delta T$  and the strain change  $\Delta\epsilon$  along the fiber can be calculated.

$$\begin{bmatrix} \Delta\nu_{B\_peak1} \\ \Delta\nu_{B\_peak2} \end{bmatrix} = \begin{bmatrix} C_{T1} & C_{\epsilon1} \\ C_{T2} & C_{\epsilon2} \end{bmatrix} \begin{bmatrix} \Delta T \\ \Delta\epsilon \end{bmatrix} \tag{1}$$

The sensor matrix can be realized by exploiting the multi-peak feature of the BGS of the dispersion compensating fiber [27], dispersion shifted fiber [28] and specialty fibers, which is due to different acoustic modes or/and different optical modes.

Ideally, by solving the inverse matrix of Equation (1), the temperature change  $\Delta T$  and the strain change  $\Delta\epsilon$  along the fiber can be calculated. The ability of accurately inverting the matrix determines measurement performance. Some sensor matrices can result in a larger error. For example, when using LEAF, the BFS-temperature/strain coefficients between different Brillouin peaks are very small, and solving the equations produces large errors [14,29]. The condition number (CN) of a matrix  $A$  is defined  $\text{cond}(A) = \|A\| \|A^{-1}\|$ , where  $\|\cdot\|$  could be any of the norms of  $A$ . In this Section, 2-norm is used to calculate  $\text{cond}(A)$  [30]. A larger CN results in a larger upper bound of the relative error [30]. Thus, a smaller CN of the sensor matrix is desirable in the sensor system. The calculated CN of the sensor matrices for the different techniques is used to provide an intuitive comparison of the measurement accuracy between the different techniques and are listed in Table 1. As can be seen, two techniques by using different fiber deployment [26], and the PM-PCF in the temperature range from 5 °C to 80 °C [31] have much smaller CNs than other techniques or other temperature ranges of the same configuration [31], indicating better achievable measurement accuracy with a smaller value of upper bound of the relative error.

**Table 1.** Summary of reported approaches to achieve discriminative sensing using specialty fibers.

Approaches	Specialty Fiber Type	Temperature Coefficient $C_T$ (MHz/°C)	Strain Coefficient $C_\epsilon$ (MHz/ $\mu\epsilon$ )	CN of the Sensor Matrix
Multi-peak BGS due to multiple acoustic modes	PCFs with a partially germanium-doped core [32,33]			
	Peak 1	0.96	0.048	
	Peak 2	1.25	0.055	346
	Large effective area fiber (LEAF) [29]			
	Peak 1 BFS	1.18	0.055	260 (peak1 BFS, peak1 BGS)
	Peak 1 BGS linewidth	-0.111	-0.00059	2580 (peak1 BFS, peak2 BFS)
Peak 2 BFS	1.2	0.055	260 (peak1 BFS, peak2 BGS)	
Peak 2 BGS linewidth	-0.118	-0.00091	270 (peak1 BGS, peak2 BFS)	
				836 (peak1 BGS, peak2 BGS)
Multi-peak BGS due to multiple optical modes	Circular core few mode fiber (FMF) [34]			
	LP <sub>01</sub>	1.0169	0.05924	221
	LP <sub>11</sub>	0.99099	0.04872	

Table 1. Cont.

Approaches	Specialty Fiber Type	Temperature Coefficient $C_T$ (MHz/°C)	Strain Coefficient $C_\epsilon$ (MHz/ $\mu\epsilon$ )	CN of the Sensor Matrix
Multi-peak BGS due to multiple acoustic modes and optical modes	Elliptical core FMF [35]			96 (LP <sub>01</sub> -P <sub>1</sub> , LP <sub>01</sub> -P <sub>2</sub> )
	LP <sub>01</sub> -P <sub>1</sub>	1.242	0.0613	107 (LP <sub>11e</sub> -P <sub>1</sub> , LP <sub>11e</sub> -P <sub>2</sub> )
	LP <sub>01</sub> -P <sub>2</sub>	1.278	0.0364	1133 (LP <sub>01</sub> -P <sub>1</sub> , LP <sub>11e</sub> -P <sub>1</sub> )
	LP <sub>11e</sub> -P <sub>1</sub>	1.287	0.0658	119 (LP <sub>01</sub> -P <sub>1</sub> , LP <sub>11e</sub> -P <sub>2</sub> )
	LP <sub>11e</sub> -P <sub>2</sub>	1.501	0.0484	88 (LP <sub>01</sub> -P <sub>2</sub> , LP <sub>11e</sub> -P <sub>1</sub> ) 538 (LP <sub>01</sub> -P <sub>2</sub> , LP <sub>11e</sub> -P <sub>2</sub> )
	Different fiber deployment [26]	1.2 ± 0.2	0.054 ± 0.7	44
	Dual core fiber [36]			
	Core 1	0.971	0.0532	95
	Core 2	0.9593	0.0729	
Multiple core/fibers	Multicore fiber (MCF) [37]			380
	Central core	1.08	0.0485	
	Outer core	1.03	0.0517	
	MCF with heterogeneous cores [38]			
	Central core	1.05 ± 0.0095	0.0485	
	Outer core	1.15 ± 0.0343	0.0485	501
BFS and birefringence	Polarization-maintaining photonic crystal fiber (PM-PCF) [31]			
	Birefringence	-40 °C to -15 °C: 27.4 -15 °C to 5 °C: 8 5 °C to 80 °C: 0	-0.154	-40 °C to -15 °C: 495 -15 °C to 5 °C: 115 5 °C to 80 °C: 7
	BFS	1.15	0.049	
BFS and fluorescence	Erbium-doped optical fiber [39]			
	Fluorescence intensity ratio	5.6 × 10 <sup>-4</sup> /°C	0	28,303
	BFS	0.87	0.0479	
Athermal/atensic optical fibers	Highly Ge dope fibers [40]	0.07	0.0214	Not applicable

The reported approaches to achieve discriminative measurement of temperature and strain or single parameter sensing measurement using specialty fibers are summarized in Table 1, based on the principles of multiple acoustic modes, multiple optical modes, multiple cores/fibers, BFS and other parameter such as birefringence or fluorescence, and athermal optical fibers. The temperature and strain coefficients of reported approaches are listed in Table 1.

*Multi-peak BGS due to multiple acoustic modes:* Firstly, the non-zero overlapping between multiple acoustic modes and fundamental optical mode field gives rise to multi-peak features on the Brillouin gain (loss) spectrum in PCFs [41]. The strain and temperature coefficients of each peak are different, enabling the discriminative sensing of two physical parameters, based on PCFs with a partially germanium-doped core as shown in Figure 2 (multi peaks are indicated by the letters a, b, c, d, e) [32,33]. Multi-peak BGS was also reported for a highly nonlinear PCF with a Ge-doped core and triangularly arranged by the F-doped buffer. However, this fiber structure does not exhibit distinct temperature and strain dependence for different peaks in the BGS and is not desirable for discriminative sensing [42]. For large effective area fiber (LEAF), such as that which has a triangle refractive index profile, the overlapping of the first three acoustic modes are comparable to the optical effective area, resulting in a multi-peak BGS. Unlike SMFs, the LEAF exhibited an observable BGS linewidth variation with strain due to greater waveguide contribution. Simultaneous detection of temperature and strain were achieved by monitoring the central frequency shift and the linewidth of the first two peaks [29].



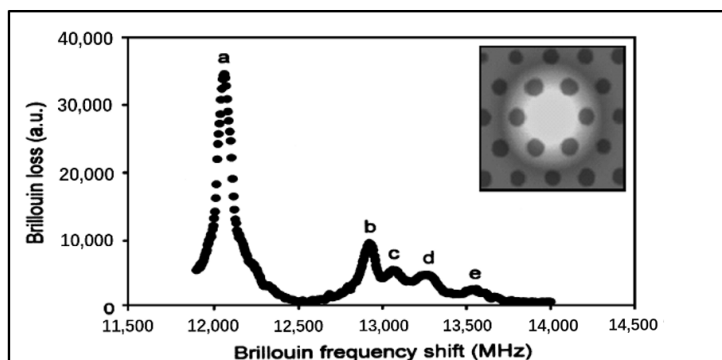


Figure 2. Multi-peak BGS due to multiple acoustic modes (indicated by the letters a, b, c, d, e). (Reprinted/Adapted) with permission from [32] © The Optical Society.

*Multi-peak BGS due to multiple optical modes:* Secondly, the optical fiber with multiple optical modes to interact with the fundamental acoustic mode, such as few-mode fiber (FMF), is another promising candidate for discriminative sensing based on different optical mode properties including different effective refractive indices, chromatic dispersion and losses. The Brillouin scattering for various linear polarized modes will create different BGSs and the corresponding BFSs will have different temperatures and strain coefficients [15]. A circular core-FMF based BOTDA was used to demonstrate the discriminative distributed measurement of temperature and strain [34]. The free-space mode launcher was used to generate specific spatial modes from the spatial light modulator (SLM) as shown in Figure 3. The BFS for LP<sub>01</sub> and LP<sub>11</sub> mode were measured and showed estimated temperature and strain sensitivities that were (1.0169 MHz/°C, 0.05924 MHz/μϵ) and (0.99099 MHz/°C, 0.04872 MHz/μϵ), respectively.

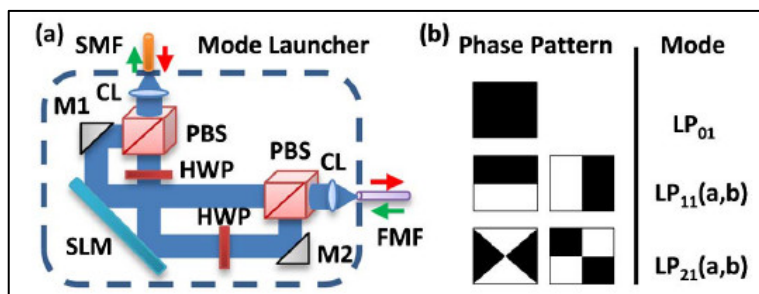


Figure 3. (a) Schematic diagram of a free-space mode launcher. (b) SLM phase patterns and the corresponding spatial modes. CL: collimating lens, M1/M2: turning mirror, HWP: half-wave plate, PBS: polarization beam splitter. (Reprinted/Adapted) with permission from [34] © The Optical Society.

*Multi-peak BGS due to multiple acoustic and optical modes:* More recently, an elliptical-core FMF based Brillouin optical time domain reflectometry (BOTDR) was reported to achieve distributed temperature and strain measurement, leveraging the multiple Brillouin peaks from the interaction between both higher-order optical modes (LP<sub>01</sub> and LP<sub>11</sub> mode) and higher-order acoustic modes. Optimum sensing performance can be achieved by choosing proper optical-acoustic mode pairs [35]. This scheme of using selected higher-order optical and modes and higher-order acoustic modes in the elliptical-core FMF offers an alternative approach to achieve temperature and strain discrimination in BOTDA, requiring a configuration of the selective mode launcher.

*Multiple core/fibers:* Thirdly, using different optical fibers or different optical fiber cores is another approach to produce BFS with different thermal and strain coefficients for simultaneous measurement of temperature and strain. In [26], the optical fibers are deployed with the configuration that the first half of the sensing is tightly bonded to

the structure to be monitored, which is sensitive to both strain and temperature, and the second half is loosely deployed and collocated to sense the temperature only. Optical fibers with dual core structure [36,43] have been reported for distributed Brillouin sensing applications. Through appropriate designing of the fiber core profile, the strain and temperature coefficients of the two sensing fiber cores are different, forming the sensing matrix equation (Equation (1)) and enable discriminative sensing of both parameters. By measuring the BGS in two cores (the central core and one of the outer cores) of a seven-core multicore fiber (MCF), the BFS in these two cores show different strain and temperature coefficients, suggesting the feasibility of using MCF based Brillouin sensing for discriminative distributed measurement of temperature and strain [37].

Further improvement can be achieved by optimizing the material and the structure of the MCF to enlarge the difference from the cores [11,37]. MCF with heterogeneous cores as shown in Figure 4 is reported to show ~70 MHz BFS difference between the central core and the outer cores, which are made from different preforms. The experimental results showed the heterogeneous cores have enlarged difference in the temperature sensitivities and indistinguishable strain sensitivities, enabling a simultaneous and discriminative dual parameter measurement [38]. Distributed bending sensing application deduced from strain measurements of the MCF based Brillouin sensors are explored subsequently [44].

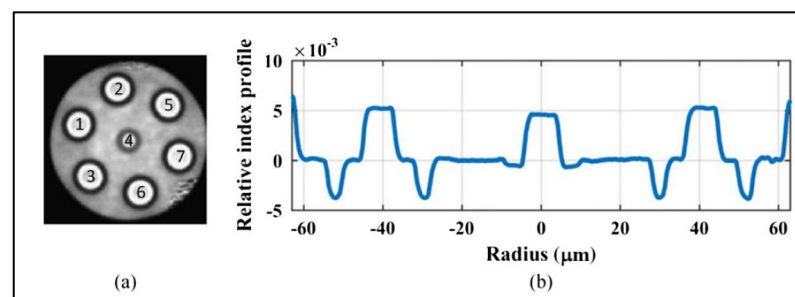


**Figure 4.** (a) Cross-sectional view of the MCF used in the experiment. (b) Relative index profile of the MCF. (Reprinted/Adapted) with permission from [38] © The Optical Society.

*BFS and birefringence/fluorescence:* The fourth approach is through simultaneous monitoring two independent physical parameters of BFS and the fiber birefringence or fluorescence. The birefringence is characterized through the measurement of the diffraction spectrum of the dynamic acoustic grating generated in SBS, or Brillouin dynamic grating (BDG). The combination of BFS and the birefringence was firstly explored using polarization-maintaining fiber (PMF), reporting a discrimination accuracy of  $3 \mu\epsilon$  and  $0.08 \text{ }^\circ\text{C}$  [45]. Compared with the conventional PMF, polarization-maintaining photonic crystal fiber (PM-PCF) acquires fiber birefringence from the non-circular core in the all-silica holey cladding structure, thus inherently possessing much less temperature sensitivity. Discriminative measurement of strain and temperature using the configuration as depicted in Figure 5, is achieved by monitoring the BFS and BDG of the PM-PCF for the temperature range of  $-40 \text{ }^\circ\text{C}$  to  $80 \text{ }^\circ\text{C}$  and the strain range of  $0\text{--}800 \mu\epsilon$ . In addition, leveraging the weak temperature sensitivity of the fiber birefringence in the temperature range from  $5 \text{ }^\circ\text{C}$  to  $80 \text{ }^\circ\text{C}$ , temperature-insensitive strain measurement is possible by using the BDG measurement alone [31]. Combination of BFS and fluorescence are used to demonstrate discriminative strain and temperature measurement in erbium-doped optical fiber [39].

*Athermal/atensic optical fibers:* If complete discrimination of temperature and strain measurement is not required, an optical fiber with immunity to one parameter is desirable for single sensing parameter measurement. It has been shown in Figure 6 that highly Ge doped fibers presented negligible temperature dependence, and the temperature coefficient even decreased to zero when removing the fiber coating, paving the way to develop athermal optical fibers for temperature-free Brillouin strain sensing [40]. Likewise, optical fibers that are insensitive to strain or atensic fibers can be designed and developed for

strain-free Brillouin temperature sensing [11]. However, these approaches to develop athermal or atensic fibers through fiber material composition optimization suffer from a significant reduction of the sensitivity to strain or temperature and in the Brillouin gain [11].

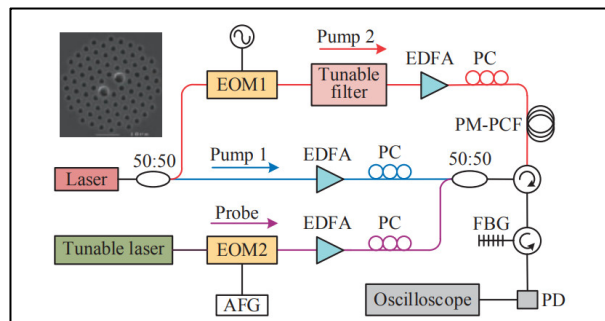


**Figure 5.** Experimental setup of distributed temperature and strain sensing using BDG and BGS. Reproduced from [31]. Copyright (2017) The Japan Society of Applied Physics.

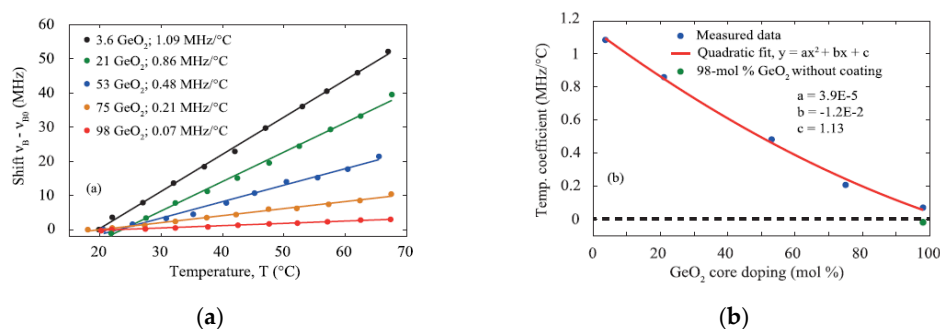


**Figure 6.** (a) Brillouin frequency shift versus the temperature increase in five different fibers; (b) SBS temperature coefficient versus GeO<sub>2</sub>-core doping levels. Reproduced with permission [40]. Licensed under a Creative Commons Attribution (CC BY) license.

### 3.3. Multiplexed Distributed Sensing Systems of BOTDA and Other Distributed Fiber Sensor Technologies

This section is focused on the reported work of specialty fibers in hybrid distributed sensing systems based on Brillouin scattering phenomena, e.g., BOTDA or BOTDR, and other DFS technologies based on Raman or Rayleigh scattering phenomena. For example, utilizing the space-division multiplexed (SDM) system configuration, MCF represent a desirable platform to develop a compact system to multiplex different distributed sensing techniques. A recent review paper introduced the research progress of MCF based hybrid distributed fiber sensor systems [46].

*Hybrid Brillouin-Rayleigh sensing:* Firstly, hybrid Brillouin-Rayleigh sensing systems have been reported to achieve simultaneous dual parameter measurements of temperature and strain, providing benefits of improved data processing and analytics for distance compensation and accuracy enhancement [47]. Standard optical fibers are used in the reported hybrid sensing system. The BFS and Rayleigh frequency shifts are measured to decouple the strain and temperature based on the following two equations, e.g., Equations (2) and (3):

$$\Delta v_B = C_{11}\Delta\epsilon + C_{12}\Delta T \tag{2}$$

$$\Delta v_R = C_{21}\Delta\epsilon + C_{22}\Delta T \tag{3}$$

$\Delta v_B$  and  $\Delta v_R$  are the shift of the Brillouin and Raman gain spectrum, respectively. The strain and temperature coefficients are denoted by  $C_{11}$  and  $C_{12}$  in Brillouin sensing system;  $C_{21}$  and  $C_{22}$  in Rayleigh sensing system, respectively. Subsequently, a more compact system of the hybrid Brillouin-Rayleigh sensing system through SDM configuration based on the MCF is reported for distributed temperature sensing as shown in Figure 7. Two spatially



separated sensors of BOTDA and  $\Phi$ -OTDR are realized in the central core and outer core, respectively. Distributed temperature sensing using the 1.565 km MCF was demonstrated to achieve 2.5 m spatial resolution, large measurement range (10 °C) by BOTDA, and 0.1 °C small temperature variation detection by  $\Phi$ -OTDR with ~0.001 °C resolution [48].

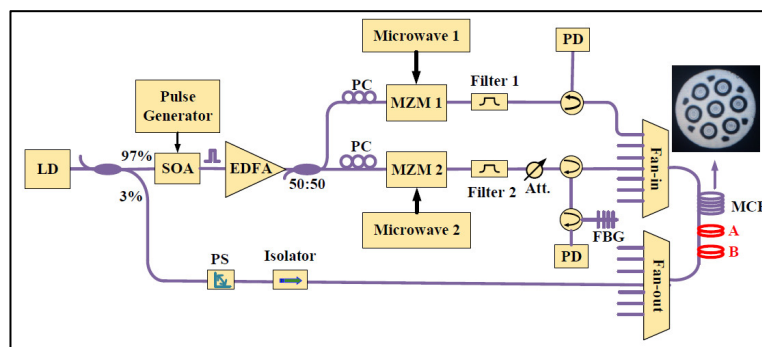


**Figure 7.** Experimental setup of the MCF based SDM hybrid BOTDA and  $\Phi$ -OTDR system. (Reprinted/Adapted) with permission from [48] © The Optical Society.

*Hybrid Brillouin-Raman sensing:* Hybrid Raman/Brillouin optical time domain reflectometry/analysis (ROTDTR and BOTDR or BOTDA) configurations using standard optical fibers are reported to realize distributed sensing of temperature and strain. The temperature measurement is determined by Raman based sensor without other cross-sensitivity from strain. Based on the temperature measurement, the strain measurement is computed and discriminated from both a strain and temperature dependent Brillouin frequency shift in the BOTDR sensor [49]. Recent advances of the hybrid Raman and Brillouin sensing systems have been reviewed, presenting promising techniques based on pulse coding to address the challenges of the tradeoff between the sensing distance and spatial resolution in the hybrid sensing system [50]. To address the incompatibility of input power requirement for hybrid ROTDR and BOTDR in standard single mode fibers, an MCF based hybrid ROTDR and BOTDR is reported for discriminative and distributed sensing of temperature and strain using a single laser source, shared pump generation devices and separate interrogation fiber channels (Figure 8). The reported system achieved worst temperature and strain resolutions about 2.2 °C and 40  $\mu\epsilon$ , respectively, in a 6 km sensing range with a 3 m spatial resolution [51]. The research progress of MCF based hybrid distributed fiber sensor systems is reviewed in [46].

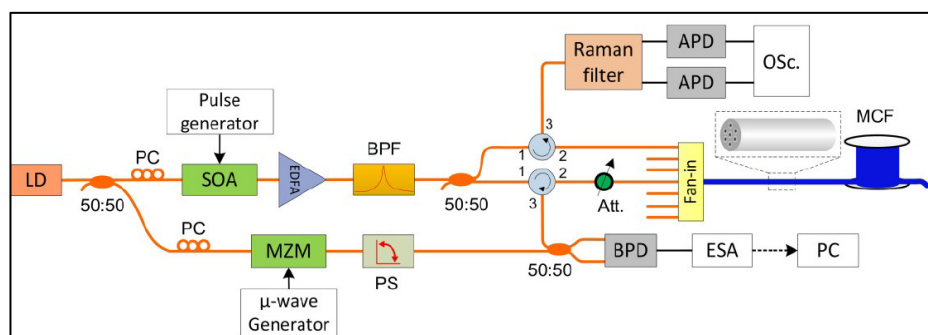


**Figure 8.** Experimental setup of the MCF based SDM hybrid ROTDR and BOTDR system. (Reprinted/Adapted) with permission from [51] © The Optical Society.

### 3.4. Distributed Sensing of Other Parameters

*Curvature sensing:* The dependence of the BFS on longitudinal strain variations (compression/elongation) is exploited to develop distributed curvature sensing using an optical fiber. Since the first sensing demonstration with an SMF (BFS ~ 1.6 MHz for a 1.5 m of

SMF wound around a rod of 25 mm diameter [52]), different optical fibers have been investigated. Among them, a few-mode fiber was used to improve the sensitivity (~5 times for a radius curvature of 0.8 cm) and to extend the range of curvature measurements (radius curvature from 0.7 cm to 3.4 cm) [53]. MCF was successfully used for demonstrating curvature radius and orientation measurements (with a BFS sensitivity of  $2.06 \text{ MHz/m}^{-1}$ ) by correlating the difference of BFS between the central core and outer six cores, paving the way to full 3D shape determination using an optical fiber [44]. The interest of an RCF, with an inner and outer core diameter of  $7.38 \mu\text{m}$  and  $15.14 \mu\text{m}$ , respectively, and a  $\Delta n_{\text{core-cladding}} \sim 0.0131$ , was demonstrated for measuring distributed small curvature radius by exploiting its excellent bending loss resistance ( $\alpha < 0.01 \text{ dB}$  for a radius of 0.5 cm) in comparison to an SMF that suffers from macro-bending losses ( $\alpha > 10 \text{ dB}$ ). In addition to a higher sensitivity than SMFs (with BFS  $\sim 32.9 \text{ MHz}$  for a radius of 0.5 cm), the RCF enables distributed curvature sensing without temperature or axial strain sensitivity by measuring its Brillouin gain variation [54], as shown in Figure 9.

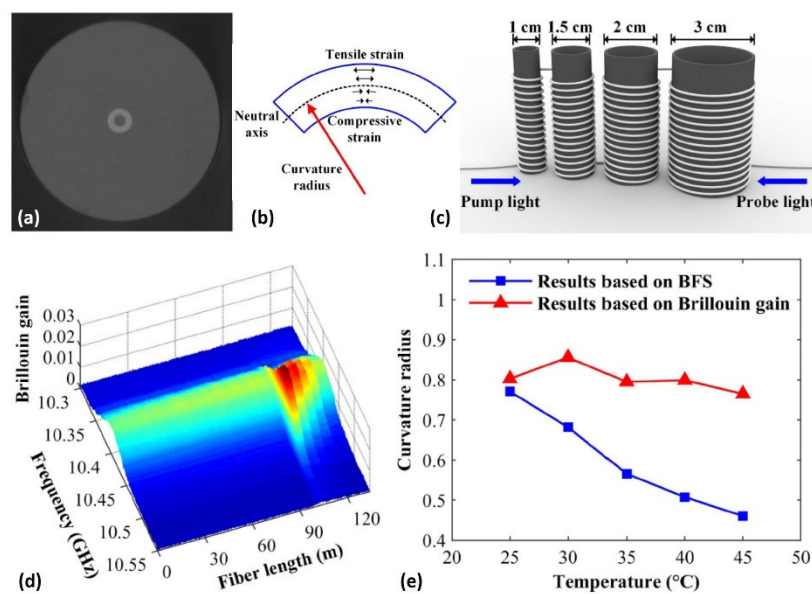


**Figure 9.** (a) Optical microscope image of the cross section of an RCF, (b) schematic illustration of strain applied in a bent fiber, (c) illustration of distributed curvature measurements by winding the RCF around different rod diameters, (d) measured Brillouin gain along the RCF including four sections where the RCF is wound. (e) Estimation of the curvature from BFS or Brillouin gain measurements versus temperature variations. Reproduced from [54], with the permission of Chinese Laser Press Publishing.

*Pressure sensing:* PM-PCF composed of only silica and air, which exhibits a very low thermal sensitivity, was used for hydrostatic pressure sensing by measuring the birefringence changes through exciting and probing the BDG (with a differential pulse-width pair Brillouin optical time domain analysis, DPP-BOTDA) [55]. A linear dependence of the Birefringence BFS difference of about  $199 \text{ MHz/MPa}$  has been measured for hydrostatic pressure from 0 to 1.1 PM with a measurement error of 0.025 MPa.

*Characterization of Fiber-Optic Parametric Amplifier (FOPA) and nonlinear optical fibers:* FOPA gain that relies on strict phase-matching conditions imposed by the four-wave mixing process was measured along the length of the highly non-linear fiber by using BOTDA in a novel scheme where the parametric amplification acts on the BOTDA pump [56]. The fluctuation measurements of the zero-dispersion wavelength (ZDW) along the highly nonlinear fiber of a FOPA was also demonstrated (with ZDW fluctuations as low as 0.02 nm along 200 m of the fiber and 2 m longitudinal resolution) [57,58]. These demonstrations offer new possibilities for precisely characterizing the chromatic dispersion along highly

nonlinear fibers, i.e., including local fluctuation, which is a key parameter for numerous nonlinear optic applications.

*Salinity measurement:* A PM-PCF with a polyimide coating was used to demonstrate salinity measurements based on BOTDA and BDG [59]. This coating shrinks in contact with a NaCl solution. A frequency shift is measured with BDG-BOTDA corresponding to a birefringence variation from modification of the hydrostatic pressure applied on the PM-PCF by the coating depending on the salinity concentration. Linear NaCl sensitivity from 30.1 MHz/(mol/L) to 139.6 MHz/(mol/L) have been reported for different coating thickness ranging from 5  $\mu\text{m}$  to 20  $\mu\text{m}$ , respectively, with a maximum salinity accuracy of 0.072 mol/L (considering a measurement uncertainty less than 10 MHz). This demonstration with a spatial resolution of 15 cm enables distributed salinity sensor with both high accuracy and high resolution.

*Refractive index measurements of liquid:* The parameters previously presented are measured by sensing the dependence of the BFS on strain variations applied on the fiber. The linear dependency of the BFS to the effective index of the propagated light into the fiber was exploited for sensing the refractive index of a liquid surrounding a side-polished optical fiber [60]. The fraction of evanescent field interacting with the liquid along the side-polished section of 3 cm was further increased by depositing a thin film with high refractive index (SU-8 photoresist,  $n = 1.56$ ), leading to a refractive index sensitivity of the BFS about 293 MHz/RIU around  $n = 1.40$ . The measurements were realized with a high spatial resolution BOFDA apparatus.

*Monitoring dihydrogen diffusion:* The diffusion of dihydrogen ( $\text{H}_2$ ) within an SMF was demonstrated with BOTDA measurements. The dependence of the BFS to  $\text{H}_2$  concentration in the silica was reported with a rate of approximately 0.21 MHz/% $\text{H}_2$  [61]. Simultaneous Rayleigh and Brillouin backscattering measurements during  $\text{H}_2$  diffusion have enabled to decorrelate the BFS induced by a refractive index variation and by a linear increase of acoustic velocity of about 5.2 (m/s)/(%mol  $\text{H}_2$ ) with  $\text{H}_2$  concentration in silica [62]. Further studies are developed to increase the BFS sensitivity to  $\text{H}_2$  concentration by inserting palladium particles ( $\text{H}_2$  sensitive material) into specialty optical fibers [63].

#### 4. Prospects and Conclusions

The flexibilities and functionalities of the specialty optical fibers have demonstrated great potential in sensor performance enhancement and application development for BOTDA systems. In this review, several key aspects of the achievements using the specialty fiber in BOTDA systems are summarized, including the Brillouin gain amplification through the integration of highly nonlinear gas medium into the hollow-core fiber, novel polarization properties of specialty fiber based BOTDA systems, sensitivity enhancements by specially coated optical fibers, discriminative sensing of temperature and strain, multiplexed distributed fiber sensing systems of BOTDA and other systems, and novel sensing parameters enabled by specialty fibers. It is believed that specialty fibers are becoming an important design and implementation considerations of the BOTDA system for distributed sensing applications. In addition, the developments of specialty fibers specially designed for a sensing application, by optimizing the topology (core shape, number of modes, multi-cores) and by associating material properties (silica/air, gas, highly Ge-doped) such as multi-material fibers, will offer new prospects for further enhancing the performance of BOTDA systems in growing applications areas such as the oil and gas industry, power industry, construction industry, transportation industry and security monitoring [9].

**Author Contributions:** Conceptualization: D.J.J.H., H.D. and H.Z.; writing-original draft preparation, D.J.J.H. and G.H.; writing-review and editing: H.D., H.Z., Q.S. and J.H. All authors have read and agreed to the published version of the manuscript.

**Funding:** This work presented in this paper is a result of the research effort through Enhancing Offshore System Productivity, Integrity and Survivability in Extreme Environments (ENSURE) programme financed by A\*STAR under its RIE 2020 Industry Alignment Fund (Grant No: A19F1a0104).

**Institutional Review Board Statement:** Not applicable.

**Informed Consent Statement:** Not applicable.

**Conflicts of Interest:** The authors declare no conflict of interest.

### Nomenclature

The symbols used in the manuscript are listed in the table below.

Symbols	Description
$\Delta\nu_{B\_peak1,2}$	The central frequency shifts of the Brillouin spectra peaks
$C_{T1,2}$	Temperature coefficients of the Brillouin peak 1, 2, respectively
$C_{\varepsilon1,2}$	Strain coefficients of the Brillouin peak 1, 2, respectively
$\Delta T$	Temperature change
$\Delta\varepsilon$	Strain change
$\Delta\nu_B$	The shift of the Brillouin gain spectrum
$\Delta\nu_R$	The shift of the Raman gain spectrum
$C_{11}$	Strain coefficient of the Brillouin sensing system
$C_{12}$	Temperature coefficient of the Brillouin sensing system
$C_{21}$	Strain coefficient of the Raman sensing system
$C_{22}$	Temperature coefficient of the Raman sensing system

### References

- Liu, Y.; Li, H.; Wang, Y.; Men, Y.; Xu, Q. Damage detection of tunnel based on the high-density cross-sectional curvature obtained using strain data from BOTDA sensors. *Mech. Syst. Signal Process.* **2021**, *158*, 107728. [[CrossRef](#)]
- Xu, J.; Dong, Y.; Li, H. Research on fatigue damage detection for wind turbine blade based on high-spatial-resolution DPP-BOTDA. In Proceedings of the SPIE 9061, Sensors and Smart Structures Technologies for Civil, Mechanical, and Aerospace Systems, San Diego, CA, USA, 10–13 March 2014. [[CrossRef](#)]
- Zhang, D.; Yang, Y.; Xu, J.; Ni, L.; Li, H. Structural Crack Detection Using DPP-BOTDA and Crack-Induced Features of the Brillouin Gain Spectrum. *Sensors* **2020**, *20*, 6947. [[CrossRef](#)]
- Jamioy, C.A.G.; Lopez-Higuera, J.M. Brillouin Distributed Fiber Sensors: An Overview and Applications. *J. Sens.* **2012**, *2012*, 204121. [[CrossRef](#)]
- Motil, A.; Bergman, A.; Tur, M. State of the art of Brillouin fiber-optic distributed sensing. *Opt. Laser Technol.* **2016**, *78*, 81–103. [[CrossRef](#)]
- Feng, C.; Kadum, J.E.; Schneider, T. *The State-of-the-Art of Brillouin Distributed Fiber Sensing*; IntechOpen: London, UK, 2019. [[CrossRef](#)]
- Dong, Y. High-Performance Distributed Brillouin Optical Fiber Sensing. *Photonic Sens.* **2021**, *11*, 69–90. [[CrossRef](#)]
- Lu, P.; Lalam, N.; Badar, M.; Liu, B.; Chorpening, B.T.; Buric, M.P.; Ohodnicki, P. Distributed optical fiber sensing: Review and perspective. *Appl. Phys. Rev.* **2019**, *6*, 041302. [[CrossRef](#)]
- Bao, X.; Zhou, Z.; Wang, Y. Review: Distributed time-domain sensors based on Brillouin scattering and FWM enhanced SBS for temperature, strain and acoustic wave detection. *PhotoniX* **2021**, *2*, 14. [[CrossRef](#)]
- Bai, Z.; Yuan, H.; Liu, Z.; Xu, P.; Gao, Q.; Williams, R.; Kitzler, O.; Mildren, R.; Wang, Y.; Lu, Z. Stimulated Brillouin scattering materials, experimental design and applications: A review. *Opt. Mater.* **2018**, *75*, 626–645. [[CrossRef](#)]
- Dragic, P.; Ballato, J. A Brief Review of Specialty Optical Fibers for Brillouin-Scattering-Based Distributed Sensors. *Appl. Sci.* **2018**, *8*, 1996. [[CrossRef](#)]
- Bastianini, F.; Di Sante, R.; Falcetelli, F.; Marini, D.; Bolognini, G. Optical Fiber Sensing Cables for Brillouin-Based Distributed Measurements. *Sensors* **2019**, *19*, 5172. [[CrossRef](#)]
- Soto, M.A.; Ramírez, J.A.; Thévenaz, L. Intensifying the response of distributed optical fibre sensors using 2D and 3D image restoration. *Nat. Commun.* **2016**, *7*, 10870. [[CrossRef](#)]
- Wang, B.; Wang, L.; Guo, N.; Zhao, Z.; Yu, C.; Lu, C. Deep neural networks assisted BOTDA for simultaneous temperature and strain measurement with enhanced accuracy. *Opt. Express* **2019**, *27*, 2530–2543. [[CrossRef](#)] [[PubMed](#)]
- Bai, Q.; Wang, Q.; Wang, D.; Wang, Y.; Gao, Y.; Zhang, H.; Zhang, M.; Jin, B. Recent Advances in Brillouin Optical Time Domain Reflectometry. *Sensors* **2019**, *19*, 1862. [[CrossRef](#)] [[PubMed](#)]
- Kobyakov, A.; Sauer, M.; Chowdhury, D. Stimulated Brillouin scattering in optical fibers. *Adv. Opt. Photonics* **2009**, *2*, 1–59. [[CrossRef](#)]
- Fortier, C.; Fatome, J.; Pitois, S.; Smektala, F.; Millot, G.; Troles, J.; Desevedavy, F.; Houizot, P.; Brillard, L.; Traynor, N. Experimental investigation of Brillouin and Raman scattering in a 2SG sulfide glass microstructured chalcogenide fiber. *Opt. Express* **2008**, *16*, 9398–9404. [[CrossRef](#)] [[PubMed](#)]
- Yang, F.; Gyger, F.; Thévenaz, L. Intense Brillouin amplification in gas using hollow-core waveguides. *Nat. Photonics* **2020**, *14*, 700–708. [[CrossRef](#)] [[PubMed](#)]



19. Yang, F.; Gyger, F.; Thévenaz, L. Giant Brillouin Amplification in Gases. *Opt. Photonics News* **2020**, *31*, 33. [[CrossRef](#)]
20. Beugnot, J.-C.; Sylvestre, T.; Alasia, D.; Maillotte, H.; Laude, V.; Monteville, A.; Provino, L.; Traynor, N.; Mafang, S.F.; Thévenaz, L. Complete experimental characterization of stimulated Brillouin scattering in photonic crystal fiber. *Opt. Express* **2007**, *15*, 15517–15522. [[CrossRef](#)] [[PubMed](#)]
21. Iyer, A.; Xu, W.; Antonio-Lopez, J.E.; Correa, R.A.; Renninger, W.H. Ultra-low Brillouin scattering in anti-resonant hollow-core fibers. *APL Photonics* **2020**, *5*, 096109. [[CrossRef](#)]
22. Dong, Y.; Qiu, L.; Lu, Y.; Teng, L.; Wang, B.; Zhu, Z. Sensitivity-Enhanced Distributed Hydrostatic Pressure Sensor Based on BOTDA in Single-Mode Fiber with Double-Layer Polymer Coatings. *J. Lightwave Technol.* **2020**, *38*, 2564–2571. [[CrossRef](#)]
23. Gu, H.; Dong, H.; Zhang, G.; He, J.; Pan, H. Effects of Polymer Coatings on Temperature Sensitivity of Brillouin Frequency Shift Within Double-Coated Fibers. *IEEE Sens. J.* **2012**, *13*, 864–869. [[CrossRef](#)]
24. Lu, X.; Soto, M.A.; Thevenaz, L. Impact of the Fiber Coating on the Temperature Response of Distributed Optical Fiber Sensors at Cryogenic Ranges. *J. Lightwave Technol.* **2017**, *36*, 961–967. [[CrossRef](#)]
25. McElhenny, J.E.; Pattnaik, R.; Toulouse, J. Polarization dependence of stimulated Brillouin scattering in small-core photonic crystal fibers. *J. Opt. Soc. Am. B* **2008**, *25*, 2107–2115. [[CrossRef](#)]
26. Bao, X.; Webb, D.J.; Jackson, D.A. Combined distributed temperature and strain sensor based on Brillouin loss in an optical fiber. *Opt. Lett.* **1994**, *19*, 141–143. [[CrossRef](#)] [[PubMed](#)]
27. Li, Z.; Yan, L.; Zhang, X.; Pan, W. Temperature and Strain Discrimination in BOTDA Fiber Sensor by Utilizing Dispersion Compensating Fiber. *IEEE Sens. J.* **2018**, *18*, 7100–7105. [[CrossRef](#)]
28. Lee, C.; Chiang, P.; Chi, S. Utilization of a dispersion-shifted fiber for simultaneous measurement of distributed strain and temperature through Brillouin frequency shift. *IEEE Photonics Technol. Lett.* **2001**, *13*, 1094–1096. [[CrossRef](#)]
29. Liu, X.; Bao, X. Brillouin Spectrum in LEAF and Simultaneous Temperature and Strain Measurement. *J. Lightwave Technol.* **2011**, *30*, 1053–1059. [[CrossRef](#)]
30. Leon, S.J. *Linear Algebra with Applications*; Pearson Prentice Hall: Upper Saddle River, NJ, USA, 2006.
31. Zhang, H.; Yuan, Z.; Liu, Z.; Gao, W.; Dong, Y. Simultaneous measurement of strain and temperature using a polarization-maintaining photonic crystal fiber with stimulated Brillouin scattering. *Appl. Phys. Express* **2016**, *10*, 012501. [[CrossRef](#)]
32. Zou, L.; Bao, X.; Chen, L. Brillouin scattering spectrum in photonic crystal fiber with a partially germanium-doped core. *Opt. Lett.* **2003**, *28*, 2022–2024. [[CrossRef](#)]
33. Zou, L.; Bao, X.; Afshar, S.; Chen, L. Dependence of the Brillouin frequency shift on strain and temperature in a photonic crystal fiber. *Opt. Lett.* **2004**, *29*, 1485–1487. [[CrossRef](#)]
34. Li, A.; Wang, Y.; Fang, J.; Li, M.-J.; Kim, B.Y.; Shieh, W. Few-mode fiber multi-parameter sensor with distributed temperature and strain discrimination. *Opt. Lett.* **2015**, *40*, 1488–1491. [[CrossRef](#)]
35. Fang, J.; Milione, G.; Stone, J.; Peng, G.; Li, M.-J.; Ip, E.; Li, Y.; Ji, P.N.; Huang, Y.-K.; Huang, M.-F.; et al. Multi-parameter distributed fiber sensing with higher-order optical and acoustic modes. *Opt. Lett.* **2019**, *44*, 1096–1099. [[CrossRef](#)]
36. Zaghoul, M.A.S.; Wang, M.; Milione, G.; Li, M.-J.; Li, S.; Huang, Y.-K.; Wang, T.; Chen, K.P. Discrimination of Temperature and Strain in Brillouin Optical Time Domain Analysis Using a Multicore Optical Fiber. *Sensors* **2018**, *18*, 1176. [[CrossRef](#)]
37. Mizuno, Y.; Hayashi, N.; Tanaka, H.; Wada, Y.; Nakamura, K. Brillouin scattering in multi-core optical fibers for sensing applications. *Sci. Rep.* **2015**, *5*, 11388. [[CrossRef](#)]
38. Zhao, Z.; Dang, Y.; Tang, M.; Li, B.; Gan, L.; Fu, S.; Wei, H.; Tong, W.; Shum, P.; Liu, D. Spatial-division multiplexed Brillouin distributed sensing based on a heterogeneous multicore fiber. *Opt. Lett.* **2016**, *42*, 171. [[CrossRef](#)]
39. Ding, M.; Mizuno, Y.; Nakamura, K. Discriminative strain and temperature measurement using Brillouin scattering and fluorescence in erbium-doped optical fiber. *Opt. Express* **2014**, *22*, 24706–24712. [[CrossRef](#)] [[PubMed](#)]
40. Deroh, M.; Sylvestre, T.; Chretien, J.; Maillotte, H.; Kibler, B.; Beugnot, J.-C. Towards athermal Brillouin strain sensing based on heavily germanium-doped core optical fibers. *APL Photonics* **2019**, *4*, 030801. [[CrossRef](#)]
41. McElhenny, J.E.; Pattnaik, R.K.; Toulouse, J.; Saitoh, K.; Koshiba, M. Unique characteristic features of stimulated Brillouin scattering in small-core photonic crystal fibers. *J. Opt. Soc. Am. B* **2008**, *25*, 582–593. [[CrossRef](#)]
42. Zou, W.; He, Z.; Hotate, K. Experimental investigation on Brillouin scattering property in highly nonlinear photonic crystal fiber with hybrid core. *Opt. Express* **2012**, *20*, 11083–11090. [[CrossRef](#)] [[PubMed](#)]
43. Li, M.-J.; Li, S.; Derick, J.A.; Stone, J.S.; Chow, B.C.; Bennett, K.W.; Sutherlin, D.M. Dual core optical fiber for distributed Brillouin fiber sensors. In Proceedings of the Asia Communications and Photonics Conference 2014, Shanghai, China, 11–14 November 2014; p. AW4I.3. [[CrossRef](#)]
44. Zhao, Z.; Soto, M.A.; Tang, M.; Thévenaz, L. Distributed shape sensing using Brillouin scattering in multi-core fibers. *Opt. Express* **2016**, *24*, 25211–25223. [[CrossRef](#)] [[PubMed](#)]
45. Zou, W.; He, Z.; Hotate, K. Complete discrimination of strain and temperature using Brillouin frequency shift and birefringence in a polarization-maintaining fiber. *Opt. Express* **2009**, *17*, 1248–1255. [[CrossRef](#)]
46. Zhao, Z.; Tang, M.; Lu, C. Distributed multicore fiber sensors. *Opto-Electron. Adv.* **2020**, *3*, 19002401–19002417. [[CrossRef](#)]
47. Kishida, K.; Yamauchi, Y.; Guzik, A. Study of optical fibers strain-temperature sensitivities using hybrid Brillouin-Rayleigh system. *Photonic Sens.* **2013**, *4*, 1–11. [[CrossRef](#)]



48. Dang, Y.; Zhao, Z.; Tang, M.; Zhao, C.; Gan, L.; Fu, S.; Liu, T.; Tong, W.; Shum, P.P.; Liu, D. Towards large dynamic range and ultrahigh measurement resolution in distributed fiber measurement resolution in distributed fiber. *Opt. Express* **2017**, *25*, 20183–20193. [[CrossRef](#)] [[PubMed](#)]
49. Alahbabi, M.N.; Cho, Y.T.; Newson, T.P. Simultaneous temperature and strain measurement with combined spontaneous Raman and Brillouin scattering. *Opt. Lett.* **2005**, *30*, 1276–1278. [[CrossRef](#)] [[PubMed](#)]
50. Muanenda, Y.; Oton, C.J.; Di Pasquale, F. Application of Raman and Brillouin Scattering Phenomena in Distributed Optical Fiber Sensing. *Front. Phys.* **2019**, *7*, 155. [[CrossRef](#)]
51. Zhao, Z.; Dang, Y.; Tang, M.; Duan, L.; Wang, M.; Wu, H.; Fu, S.; Tong, W.; Shum, P.P.; Liu, D. Spatial-division multiplexed hybrid Raman and Brillouin optical time-domain reflectometry based on multi-core fiber. *Opt. Express* **2016**, *24*, 25111–25118. [[CrossRef](#)]
52. Minardo, A.; Bernini, R.; Zeni, L. Bend-Induced Brillouin Frequency Shift Variation in a Single-Mode Fiber. *IEEE Photonics Technol. Lett.* **2013**, *25*, 2362–2364. [[CrossRef](#)]
53. Wu, H.; Tang, M.; Wang, M.; Zhao, C.; Zhao, Z.; Wang, R.; Liao, R.; Fu, S.; Yang, C.; Tong, W.; et al. Few-mode optical fiber based simultaneously distributed curvature and temperature sensing. *Opt. Express* **2017**, *25*, 12722. [[CrossRef](#)]
54. Shen, L.; Wu, H.; Zhao, C.; Zhang, R.; Tong, W.; Fu, S.; Tang, M. Distributed curvature sensing based on a bending loss-resistant ring-core fiber. *Photonics Res.* **2020**, *8*, 165. [[CrossRef](#)]
55. Teng, L.; Dong, Y.K.; Zhou, D.; Jiang, T.; Zhou, D.W. Temperature-compensated distributed hydrostatic pressure Brillouin sensor using a thin-diameter and polarization-maintaining photonics crystal fiber. In Proceedings of the Asia-Pacific Optical Sensors Conference 2016, Shanghai, China, 11–14 October 2016; p. W4A.55. [[CrossRef](#)]
56. Vedadi, A.; Alasia, D.; Lantz, E.; Maillotte, H.; Thevenaz, L.; Gonzalez-Herraez, M.; Sylvestre, T. Brillouin Optical Time-Domain Analysis of Fiber-Optic Parametric Amplifiers. *IEEE Photonics Technol. Lett.* **2007**, *19*, 179–181. [[CrossRef](#)]
57. Alishahi, F.; Vedadi, A.; Denisov, A.; Soto, M.A.; Mehrany, K.; Bres, C.S.; Thevenaz, L. Highly sensitive dispersion map extraction from highly nonlinear fibers using BOTDA probing of parametric amplification. In Proceedings of the 2013 Conference on Lasers & Electro-Optics Europe & International Quantum Electronics Conference CLEO EUROPE/IQEC, Munich, Germany, 12–16 May 2013; p. 1. [[CrossRef](#)]
58. Alishahi, F.; Vedadi, A.; Shoaie, A.; Mehrany, K.; Salehi, J.A. Low resolution distributed measurement of fiber optical parametric amplifiers gain. In Proceedings of the Optical Fiber Communication Conference 2012, Los Angeles, CA, USA, 4–8 March 2012; p. JW2A.30.
59. Zhang, H.; Teng, L.; Dong, Y. Distributed Salinity Sensor with a Polyimide-Coated Photonic Crystal Fiber Based on Brillouin Dynamic Grating. *J. Lightwave Technol.* **2020**, *38*, 5219–5224. [[CrossRef](#)]
60. Bernini, R.; Persichetti, G.; Catalano, E.; Zeni, L.; Minardo, A. Refractive index sensing by Brillouin scattering in side-polished optical fibers. *Opt. Lett.* **2018**, *43*, 2280–2283. [[CrossRef](#)] [[PubMed](#)]
61. Delepine-Lesoille, S.; Bertrand, J.; Lablonde, L.; Pheron, X. Distributed Hydrogen Sensing with Brillouin Scattering in Optical Fibers. *IEEE Photonics Technol. Lett.* **2012**, *24*, 1475–1477. [[CrossRef](#)]
62. Leparmentier, S.; Auguste, J.-L.; Humbert, G.; Pilorget, G.; Lablonde, L.; Delepine-Lesoille, S. Study of the hydrogen influence on the acoustic velocity of single-mode fibers by Rayleigh and Brillouin backscattering measurements. In Proceedings of the 24th International Conference on Optical Fibre Sensors, Curitiba, Brazil, 28 September–2 October 2015; Volume 9634, p. 963432. [[CrossRef](#)]
63. Delepine-Lesoille, S.; Girard, S.; Landolt, M.; Bertrand, J.; Planes, I.; Boukenter, A.; Marin, E.; Humbert, G.; Leparmentier, S.; Auguste, J.-L.; et al. France's State of the Art Distributed Optical Fibre Sensors Qualified for the Monitoring of the French Underground Repository for High Level and Intermediate Level Long Lived Radioactive Wastes. *Sensors* **2017**, *17*, 1377. [[CrossRef](#)] [[PubMed](#)]